



Proceedings of the Seventh International Conference on
Parallel, Distributed, GPU and Cloud Computing for Engineering
Edited by: P. Iványi, F. Magoulès and B.H.V. Topping
Civil-Comp Conferences, Volume 4, Paper 2.2
Civil-Comp Press, Edinburgh, United Kingdom, 2023
doi: 10.4203/ccc.4.2.2
©Civil-Comp Ltd, Edinburgh, UK, 2023

Schwarz domain decomposition algorithms to solve radiative transfer equation

E. Straková and T. Brzobohatý

IT4Innovations, VSB - Technical University of Ostrava, Czech
Republic

Abstract

In this paper, the solving radiative transfer equation by the optimized Schwarz method is presented. The optimized Schwarz method is applied as a preconditioner for the Krylov subspace method to improve the convergence rate. The discrete ordinate and mixed finite element methods are used for the angular and spatial discretization. The numerical scalability of Schwarz-type preconditioners is discussed for the different parameters of the radiative transfer equation.

Keywords: radiative transfer equation, domain decomposition, restrictive additive Schwarz preconditioner, optimized Schwarz preconditioner, discrete ordinate method, streamline upwind Petrov-Galerkin finite element method

1 Introduction

Radiation heat transfer is an essential problem in many areas of engineering. The general energy equation describing the radiation heat transfer contains the local divergence of radiative flux (see [1]). When dealing with the absorbing-emitting-scattering medium, it is necessary to evaluate the radiative flux by solving the radiative transfer

equation (RTE). This equation determines the intensity of the radiation field.

In this paper, we solved the radiative transfer equation using angular discretization (for s) and spatial discretization (for x). The discrete ordinate method (DOM) handles the angular discretizations by replacing the integral over the unit sphere by a quadrature rule or a weighted summation. This method was first introduced by Chandrasekhar [2]. Ever since, it has been widely used and developed [3–6].

The spatial discretization is performed using the Finite Element Method (FEM), which is attractive because it couples directly with FEM solutions to the energy equation. Spurious oscillations can occur if the standard Galerkin FEM is used to solve RTE. The Streamline Upwind Petrov-Galerkin FEM (SUPG-FEM) is used to avoid this. This method has certain advantages over the other methods [7]. As for the matrix assembling process, it is more time efficient to use the mixed finite element [9]. The mixed FEM matrix is banded, while the standard FEM matrix has a block structure.

Using the FEM-DOM discretization, a large sparse linear system is obtained. The size of the system of equations can be a bottleneck for the limited memory options of the computer. In such cases, we can apply Domain Decomposition (DD) methods. The basic idea of DD methods is to divide the original problem into several suitable subproblems [10, 11]. We can use parallel computation in domain decomposition methods to provide good preconditioners for the Krylov subspace method. Two basic Schwarz domain decomposition methods are used: the additive and the multiplicative. By introducing the different boundary conditions, the improved variants of those preconditioners can be obtained, the so-called optimized Schwarz method, already introduced for various problems (see [14–16]). Since this method was used to reduce the iteration counts, we propose using the optimized Schwarz method for the radiative transfer equation. The numerical experiments focused on the numerical scalability of the classical and optimized Schwarz method for the different parameters of the radiative transfer equation are presented.

2 The radiative transfer equation

Radiative transfer describes how electromagnetic radiation is transmitted through a participating medium. The radiative energy can be defined by the radiative intensity $I(\mathbf{x}, \mathbf{s}, t)$, which is a function of the position \mathbf{x} , the direction \mathbf{s} , and the time t . Finding the radiative intensity $I(\mathbf{x}, \mathbf{s})$ in a participating medium requires the solution of the RTE. In this paper, we consider the monochromatic steady-state radiative transfer equation described in the form

$$(\mathbf{s} \cdot \nabla + \kappa + \sigma_s) I(\mathbf{x}, \mathbf{s}) = \frac{\sigma_s}{4\pi} \int_{s'=4\pi} I(\mathbf{x}, \mathbf{s}') \Phi(\mathbf{s}, \mathbf{s}') d\mathbf{s}' + \kappa I_b(T) \quad \forall \mathbf{x} \in \Omega, \mathbf{s} \in \mathcal{S} \quad (1)$$

where κ, σ_s are absorption and scattering coefficients, respectively. I_b is Planck's

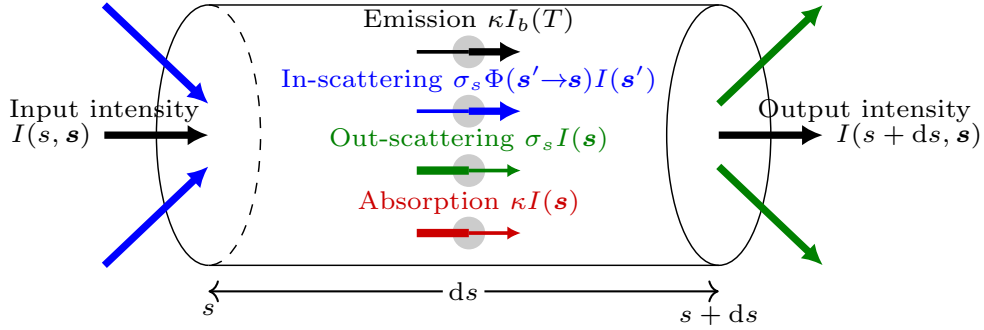


Figure 1: Change in the radiation intensity by absorption, scattering, and emission processes.

blackbody intensity, \mathcal{S} denotes the unit sphere, and Φ is the scattering phase function, which describes the distribution of scattered energy coming from direction \mathbf{s}' into direction \mathbf{s} . Figure 1 shows the change in intensity along a path increment $d\mathbf{s}$ caused by losses due to attenuation by scattering and absorption, gain by emission from the medium, and gain by in-scattering of intensity arriving from other directions.

For the opaque and diffuse emitting wall, the inflow radiative intensity is given as

$$I_w(\mathbf{x}_w, \mathbf{s}) = \varepsilon_w I_b(T_w) + \frac{1 - \varepsilon_w}{\pi} \int_{\mathbf{n}_w \cdot \mathbf{s}' > 0} I(\mathbf{x}_w, \mathbf{s}') \mathbf{n}_w \cdot \mathbf{s}' d\mathbf{s}' \quad \forall (\mathbf{x}_w, \mathbf{s}) \in \Gamma^- \quad (2)$$

where ε_w is the wall emissivity, \mathbf{n}_w is the outward unit normal vector and Γ^- is the inflow boundary, i.e $\Gamma^- = \{(\mathbf{x}, \mathbf{s}) \mid \mathbf{x} \in \partial\Omega, \mathbf{s} \cdot \mathbf{n} < 0\}$.

3 Solving the radiative transfer equation using DOM and FEM

The DOM is based on the approximation of the angular space $\mathbf{s} \in \mathcal{S}$ by a set of m discrete directions $(\mathbf{s}_1, \mathbf{s}_2, \dots, \mathbf{s}_m)$. Therefore, the RTE is solved for this set of directions and the integrals over direction are replaced by numerical quadratures, that is

$$\int_{\mathcal{S}} I(\mathbf{x}, \mathbf{s}) d\mathbf{s} = \sum_{i=1}^m I_i(\mathbf{x}) w_i \quad (3)$$

where w_i are the quadrature weights associated with the direction \mathbf{s}_i . The choice of quadrature scheme is arbitrary, although restrictions on the directions \mathbf{s}_i and quadrature weights w_i may arise from the idea of preserving symmetry and satisfying certain conditions. For radiative transfer calculation, the level symmetric quadrature sets S_N developed by Lathrop and Carlson [8] are still the most widely and commonly used sets. In this quadrature, the direction cosines of the discrete directions (η, μ, ξ) are arranged on $N/2$ levels relative to each vertex of the first octant of a unit sphere (see

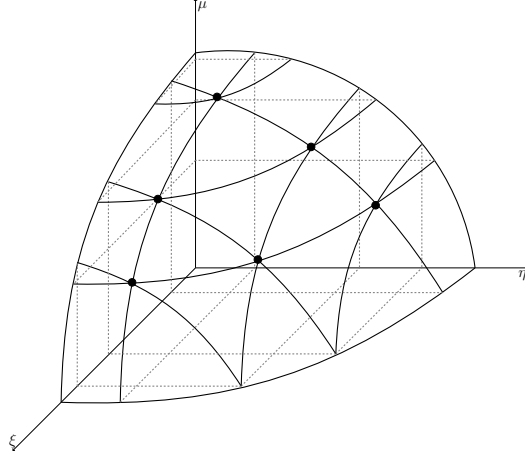


Figure 2: Point arrangement for S_6 level symmetric quadrature sets.

Figure 2). The order of an S_N quadrature represents the number of different direction cosines for every axis.

The i th equation in the set of m equations takes the form

$$RTE_i(I_1, \dots, I_m) = (\mathbf{s}_i \cdot \nabla + \kappa + \sigma_s) I_i(\mathbf{x}) - \sigma_s \sum_{j=1}^m w_j I_j(\mathbf{x}) \Phi_{i,j} - \kappa I_b(T) = 0. \quad (4)$$

Since the RTE is a convection-dominant equation, the spatial discretization using the standard Galerkin FEM appears unstable. The standard Galerkin FEM and the SUPG-FEM are compared in Figure 3, where the radiative intensity for the direction $\mathbf{s} = (0.6815, -0.6815)$ is shown. The radiative transfer in the unit square medium is considered without scattering, and the absorption coefficient is non-zero ($\kappa = 10$) only for $x + y > 1.6$. The inflow boundary condition is prescribed at the left and the top walls with an intensity of unity.

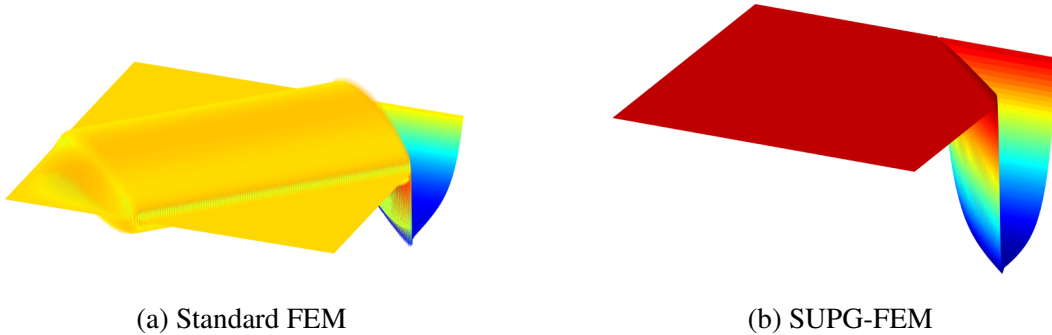


Figure 3: Radiative intensity with the spurious wiggles for the non-scattering radiative transfer problem with the inflow boundary condition.

To obtain the SUPG discrete variational formulation, each $RTE_i(I_1, \dots, I_m)$ is

multiplied by the SPUG test function $v^h + \gamma \mathbf{s}_i \nabla v^h$ and then integrated over the domain Ω^h . The additional term $\gamma \mathbf{s}_i \nabla v^h$ adds artificial dissipation but vanishes for all sufficiently smooth solutions. The suitable stabilizing coefficient γ , obtained by the numerical experiments, can be expressed as

$$\gamma = \sqrt{\frac{h^2 m}{4m + hm(\kappa + \sigma_s)^2 + 4h\sigma_s}}, \quad (5)$$

where h is the mesh size and m is number of the discrete directions.

For the reason of easier parallelization and faster matrix assembly, the mixed FEM is used for solving the RTE. Equation (4) can be reformulated in its equivalent mixed form, which reads as

$$\mathbf{S} \cdot \nabla \mathbf{I} + \Phi \mathbf{I} = \kappa I_b(T) \mathbf{1}, \quad (6)$$

where

$$\mathbf{I} = \begin{bmatrix} I_1 \\ \vdots \\ I_m \end{bmatrix}, \quad \mathbf{S} = \begin{bmatrix} \mathbf{s}_1 \\ \vdots \\ \mathbf{s}_m \end{bmatrix}, \quad (7)$$

$$\Phi = \begin{bmatrix} \beta - \sigma_s w_1 \Phi_{1,1} & -\sigma_s w_2 \Phi_{1,2} & \cdots & -\sigma_s w_m \Phi_{1,m} \\ -\sigma_s w_1 \Phi_{2,1} & \beta - \sigma_s w_2 \Phi_{2,2} & \cdots & -\sigma_s w_m \Phi_{2,m} \\ \vdots & \vdots & \ddots & \vdots \\ -\sigma_s w_1 \Phi_{m,1} & -\sigma_s w_2 \Phi_{m,2} & \cdots & \beta - \sigma_s w_m \Phi_{m,m} \end{bmatrix}.$$

The mixed SUPG discrete variational formulation consists in finding \mathbf{I}^h such that $\mathbf{a}(\mathbf{I}^h, \mathbf{v}^h) = \mathbf{b}(\mathbf{v}^h)$ for all \mathbf{v}^h from the appropriate vectorial Sobolev space. The vectorial bilinear functional \mathbf{a} and the linear functional \mathbf{b} takes the form

$$\begin{aligned} \mathbf{a}(\mathbf{I}^h, \mathbf{v}^h) &= \int_{\Omega_h} (\mathbf{S} \cdot \nabla \mathbf{v}^h)^T (-\mathbf{I}^h + \gamma \mathbf{S} \cdot \nabla \mathbf{I}^h) + (\Phi \mathbf{I}^h)^T (\mathbf{v}^h + \gamma \mathbf{S} \cdot \mathbf{v}^h) \, d\mathbf{x} \\ &\quad + \int_{\partial\Omega_h} (\mathbf{S} \cdot \mathbf{n} : \mathbf{H}_{[\mathbf{S} \cdot \mathbf{n} > 0]} : \mathbf{I}^h)^T \mathbf{v}^h \, d\mathbf{x} \\ \mathbf{b}(\mathbf{v}^h) &= \int_{\Omega_h} (\kappa I_b \mathbf{1})^T (\mathbf{v}^h + \gamma \mathbf{S} \cdot \nabla \mathbf{v}^h) \, d\mathbf{x} - \int_{\partial\Omega_h} (\mathbf{S} \cdot \mathbf{n} : \mathbf{H}_{[\mathbf{S} \cdot \mathbf{n} < 0]} : \mathbf{I}_{\text{wall}})^T \mathbf{v}^h \, d\mathbf{x}. \end{aligned} \quad (8)$$

The linear system assembled by the standard FEM is equivalent to the system assembled by the mixed FEM, i.e. they contain the same number of coefficients and their values. The difference occurs in the sparsity pattern. The standard FEM matrices have a block structure, while the mixed FEM matrices are sparse. The matrix structures arising from both methods with four discrete directions are compared in Figure 4.

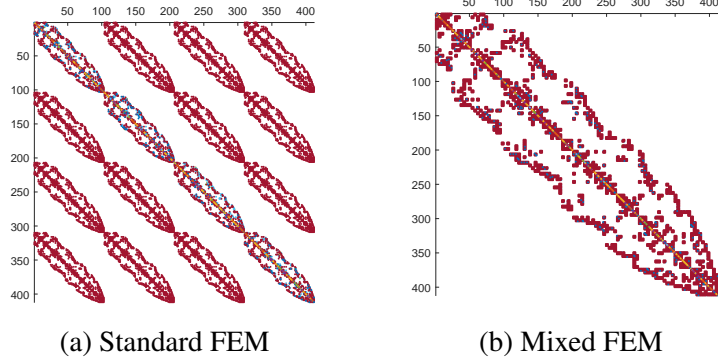


Figure 4: Sparsity pattern of the standard and mixed FEM.

4 Solving the radiative transfer equation using Schwarz methods

As a consequence of the FEM-DOM discretization, a linear system of the form $\mathbf{A}\mathbf{I} = \mathbf{b}$ has to be solved. The assembled matrix \mathbf{A} is large, sparse and nonsymmetric. The resulting linear systems can be efficiently solved using a Krylov subspace method such as the preconditioned generalized minimal residual method (GMRES). In this paper, we deal with the class of additive Schwarz preconditioners, which contains parallelism and is particularly suitable for implementation on parallel computers.

4.1 Classical Schwarz method

For simplicity, consider a unit square computational domain decomposed into $N = M \times M$ rectangular subdomains. Let $\{\hat{\Omega}_j\}$ be the non-overlapping partition of the unknowns. We obtain an overlapping decomposition $\{\Omega_j\}$ by extending these sets with an overlap of width $\delta = Ch$. Let R_j denote the vectorial restriction operator that returns the vector of coefficients of interior nodes of the desired subdomain Ω_j and D_j the vectorial partition unity operator, which satisfy $I_d = R_j^T D_j R_j$. The classical restrictive additive one-level Schwarz (RAS) preconditioner is

$$M_{RAS}^{-1} = \sum_{j=1}^N R_j^T D_j \mathbf{A}_j^{-1} R_j \quad (9)$$

where $\mathbf{A}_j = R_i \mathbf{A} R_j^T$. One drawback of the one-level method is that the number of iterations depends on the number of subdomains. This problem can be fixed by adding the coarse space with nodes (iH, jH) , where $H = 1/M$. We obtain the two-level RAS preconditioner by expanding the one-level RAS with the added relation $R_0^T (\mathbf{A}_0)^{-1} R_0$, where R_0 is the vectorial interpolation from the coarse to the fine mesh. Another type of Schwarz method is the hybrid method which is expected to take advantage of both additive and multiplicative Schwarz methods. The hybrid restrictive additive Schwarz

preconditioner is given by

$$M_{HY,RAS}^{-1} = R_0^T \mathbf{A}_0^{-1} R_0 + (I - R_0^T \mathbf{A}_0^{-1} R_0 \mathbf{A}) M_{RAS}^{-1}. \quad (10)$$

4.2 Optimized Schwarz method

The RAS method uses Dirichlet conditions at the interfaces between subdomains. A major improvement of the RAS method comes from using other interface conditions. The advantage of these methods is faster convergence and ensuring the convergence for non-overlapping domain decomposition. The second-order optimized restrictive additive one-level Schwarz (O2RAS) preconditioner is

$$M_{O2RAS}^{-1} = \sum_{j=1}^N R_j^T D_j \tilde{\mathbf{A}}_j^{-1} R_j. \quad (11)$$

The optimized subdomain matrices take the form

$$\tilde{\mathbf{A}}_j = \mathbf{A}_j - M_{\Gamma}^p + M_{\Gamma}^q. \quad (12)$$

Here \mathbf{A}_j are local matrices of the problem and $M_{\Gamma}^p, M_{\Gamma}^q$ are interface matrices

$$[M_{\Gamma}^p]_{j,l} = \int_{\partial\Omega_j \setminus \partial\Omega} \begin{bmatrix} p_1 \phi_1^j \phi_1^l & & \\ & \ddots & \\ & & p_m \phi_m^j \phi_m^l \end{bmatrix} d\mathbf{x}, \quad (13)$$

$$[M_{\Gamma}^q]_{j,l} = \int_{\partial\Omega_j \setminus \partial\Omega} \begin{bmatrix} q_1 \frac{\partial \phi_1^j}{\partial \boldsymbol{\tau}} \phi_1^l & & \\ & \ddots & \\ & & q_m \frac{\partial \phi_m^j}{\partial \boldsymbol{\tau}} \phi_m^l \end{bmatrix} d\mathbf{x}, \quad (14)$$

where $\boldsymbol{\tau}$ is the tangential direction to the interface, \mathbf{p} and \mathbf{q} are the unknown optimized parameters. The functions ϕ_i^j, ϕ_i^l are the basis functions associated with the nodes j, l in the domain Ω_j and the direction i . To obtain optimal performance of the Schwarz method, we have to solve the min-max problem

$$\min_{\mathbf{p}, \mathbf{q} \in \mathbb{R}^m} \left(\max_{0 \leq k \leq \frac{\pi}{h}} \max \left(\rho(\mathcal{T}_1^{-1} \mathcal{T}_2 \mathcal{T}_3^{-1} \mathcal{T}_4), \rho(\mathcal{T}_3^{-1} \mathcal{T}_4 \mathcal{T}_1^{-1} \mathcal{T}_2) \right) \right), \quad (15)$$

where

$$\begin{aligned} \mathcal{T}_1 &= \left[e^{\lambda_1^+ \delta} \mathcal{M}^+(\lambda_1^+, \mathbf{p}, \mathbf{q}, k) \mathbf{V}_1^+(k), \dots, e^{\lambda_m^+ \delta} \mathcal{M}^+(\lambda_m^+, \mathbf{p}, \mathbf{q}, k) \mathbf{V}_m^+(k) \right] \\ \mathcal{T}_2 &= \left[e^{\lambda_1^- \delta} \mathcal{M}^+(\lambda_1^-, \mathbf{p}, \mathbf{q}, k) \mathbf{V}_1^-(k), \dots, e^{\lambda_m^- \delta} \mathcal{M}^+(\lambda_m^-, \mathbf{p}, \mathbf{q}, k) \mathbf{V}_m^-(k) \right] \\ \mathcal{T}_3 &= \left[\mathcal{M}^-(\lambda_1^-, \mathbf{p}, \mathbf{q}, k) \mathbf{V}_1^-(k), \dots, \mathcal{M}^-(\lambda_m^-, \mathbf{p}, \mathbf{q}, k) \mathbf{V}_m^-(k) \right] \\ \mathcal{T}_4 &= \left[\mathcal{M}^-(\lambda_1^+, \mathbf{p}, \mathbf{q}, k) \mathbf{V}_1^+(k), \dots, \mathcal{M}^-(\lambda_m^+, \mathbf{p}, \mathbf{q}, k) \mathbf{V}_m^+(k) \right] \end{aligned} \quad (16)$$

and

$$\begin{aligned} \mathcal{M}^\pm(\lambda, \mathbf{p}, \mathbf{q}, k) = & \pm \lambda \gamma \begin{bmatrix} -s_{1,1}^2 & & \\ & \ddots & \\ & & -s_{m,1}^2 \end{bmatrix} \pm \gamma k i \begin{bmatrix} s_{1,1} s_{1,2} & & \\ & \ddots & \\ & & s_{m,1} s_{m,2} \end{bmatrix} \\ \pm & \begin{bmatrix} s_{1,1} & & \\ & \ddots & \\ & & s_{m,1} \end{bmatrix} \pm \gamma \begin{bmatrix} -s_{1,1} & \cdots & -s_{m,1} \\ \vdots & & \vdots \\ -s_{1,1} & \cdots & -s_{m,1} \end{bmatrix} \Phi + \begin{bmatrix} k i q_1 - p_1 & & \\ & \ddots & \\ & & k i q_m - p_m \end{bmatrix}. \end{aligned} \quad (17)$$

In equation (16), λ_i^+ and V_i^+ (or λ_i^- and V_i^-) are the eigenvalues with positive real part (or negative real part) and their corresponding eigenvectors of the quadratic eigenvalue problem

$$\begin{aligned} & \left(\begin{array}{c} \left(-\gamma \begin{bmatrix} s_{1,1}^2 & & \\ & \ddots & \\ & & s_{m,1}^2 \end{bmatrix} \lambda^2 + 2\gamma k i \begin{bmatrix} s_{1,1} s_{1,2} & & \\ & \ddots & \\ & & s_{m,1} s_{m,2} \end{bmatrix} \lambda + \begin{bmatrix} s_{1,1} & & \\ & \ddots & \\ & & s_{m,1} \end{bmatrix} \lambda \right. \\ + \gamma \begin{bmatrix} -s_{1,1} & \cdots & -s_{m,1} \\ \vdots & & \vdots \\ -s_{1,1} & \cdots & -s_{m,1} \end{bmatrix} \Phi \lambda + \Phi + \gamma k^2 \mathbf{1} \begin{bmatrix} s_{1,2}^2 & & \\ & \ddots & \\ & & s_{m,2}^2 \end{bmatrix} - k i \begin{bmatrix} s_{1,2} & & \\ & \ddots & \\ & & s_{m,2} \end{bmatrix} \\ \left. + \gamma k i \begin{bmatrix} s_{1,1} & \cdots & s_{m,1} \\ \vdots & & \vdots \\ s_{1,1} & \cdots & s_{m,1} \end{bmatrix} \Phi \right) \mathbf{V} = \mathbf{0}. \end{array} \right) \quad (18) \end{aligned}$$

5 Numerical experiments

This section presents numerical results for two-level hybrid versions of RAS and O2RAS preconditioners. We will look at how the convergence rate depends on the overlap, the mesh size and the number of subdomains. We consider the unit square domain and the radiative transfer problem (6) with the opaque and diffuse emitting walls ($\varepsilon_{wall} = 0.5$, $T_{wall} = 20K$). For our experiments, we concentrated on the following choices of constant coefficient:

- **Test problem 1** $\kappa = 5$, $\sigma_s = 10$, $T = 300K$, $\phi_{i,j} = 1$
- **Test problem 2** $\kappa = 0.2$, $\sigma_s = 0.1$, $T = 300K$, $\phi_{i,j} = 1$

The overlapping subdomain partition is obtained by extending the coarse elements by adding layers of fine elements. Iteration counts are provided using $M_{HY,RAS}^{-1}$ and $M_{HY,O2RAS}^{-1}$ respectively in the GMRES method without restarts to solve **Test problem 1** and **Test problem 2**. The iterations are stopped after reducing the Euclidean norm of the preconditioned residual by a factor 10^{-6} . Iteration counts are shown in

1/h	32	64	128	32	64	128	32	64	128	32	64	128
Overlap	H = 1/2			H = 1/4			H = 1/8			H = 1/16		
h	11	13	16	9	12	13	8	9	12	5	8	9
2h	9	10	13	8	8	11	6	7	8	x	6	7
4h	8	9	11	6	8	9	x	5	8	x	x	6
8h	6	8	8	x	6	8	x	x	6	x	x	x

Table 1: Iteration counts of GMRES with $M_{HY,RAS}^{-1}$ preconditioner for solving Test Problem 1.

1/h	32	64	128	32	64	128	32	64	128	32	64	128
Overlap	H = 1/2			H = 1/4			H = 1/8			H = 1/16		
h	6	7	8	5	6	8	4	5	6	4	4	5
2h	5	6	7	4	5	6	4	4	4	x	4	4
4h	4	4	5	4	4	5	x	5	5	x	x	5
8h	4	4	4	x	4	5	x	x	5	x	x	x

Table 2: Iteration counts of GMRES with $M_{HY,O2RAS}^{-1}$ preconditioner for solving Test Problem 1.

Table 1 - 4 as functions of the fine mesh size and the overlap δ , for different partitions. Entries with the same overlapping factor $\frac{H}{\delta}$ are in the same colour. In both test problems, Table 2 and Table 4 show that the number of iterations is lower in the GMRES method with hybrid O2RAS preconditioner compared to the GMRES method with hybrid RAS preconditioner. The resulting tables 1 and 2 of the **Test problem 1** show that similar iteration counts are found in each diagonal of the tables corresponding to the same value of $\frac{H}{\delta}$. This shows that if the overlapping factor is kept constant, iteration counts are independent of the mesh parameters H and h . A different behaviour occurs in **Test problem 2**. Table 3 and Table 4 show that the iteration count depends on H and h for a constant value of the overlapping factor. In **Test problem 2**, the GMRES with hybrid RAS or O2RAS preconditioners performs better when the number of subdomains is not too large.

6 Conclusion

The FEM-DOM method was briefly described to solve the radiative transfer equation. The Schwarz-type preconditioners were used to obtain the advantage of parallel computation. The optimized Schwarz preconditioner appears to be more appropriate due

1/h	32	64	128	32	64	128	32	64	128	32	64	128
Overlap	H = 1/2			H = 1/4			H = 1/8			H = 1/16		
h	9	10	11	14	17	21	18	23	35	14	25	39
2h	7	7	8	11	13	17	14	18	28	x	20	29
4h	7	7	7	10	11	14	x	16	20	x	x	29
8h	6	7	7	x	11	12	x	x	20	x	x	x

Table 3: Iteration counts of GMRES with $M_{HY,RAS}^{-1}$ preconditioner for solving Test Problem 2.

1/h	32	64	128	32	64	128	32	64	128	32	64	128
Overlap	H = 1/2			H = 1/4			H = 1/8			H = 1/16		
h	5	5	7	7	9	11	10	13	22	6	16	24
2h	5	5	5	7	8	8	6	9	19	x	8	17
4h	4	5	5	7	7	8	x	11	12	x	x	15
8h	4	5	5	x	6	7	x	x	11	x	x	x

Table 4: Iteration counts of GMRES with $M_{HY,O2RAS}^{-1}$ preconditioner for solving Test Problem 2.

to the reduction of the iteration count. The iteration counts of the Schwarz preconditioner were tested for different values of the overlapping factor. For some choices of the RTE parameters, the iteration counts are independent of the mesh size h and the subdomain size H for the constant value of the overlapping factor.

References

- [1] M.F. Modest, “Radiative Heat Transfer”, Academic press, 2013.
- [2] S. Chandrasekhar, “Radiative Transfer”, Oxford, Clarendon Press, 1950 .
- [3] W.A. Fiveland, “Discrete ordinate methods for radiative heat transfer in isotropically and anisotropically scattering media”, Journal of Heat Transfer - Transactions of the ASME, 109(3), 809-812, 1987.
- [4] K.D. Lathrop, “Use of discrete-ordinates methods for solution of photon transport problems”, Nuclear Science and Engineering, 24(4), 381-388, 1966.
- [5] W.A. Fiveland, “Discrete-ordinates solutions of the radiative transport equation for rectangular enclosures”, Journal of heat transfer, 106(4), 699-706, 1984.
- [6] J.S. Truelove, “Discrete-ordinate solutions of the radiation transport equation”, Journal of Heat Transfer - Transactions of the ASME, 109(4), 1987.
- [7] D.L. Hardy, Y. Favennec, B. Rousseau, “Solution of the 2-d steady-state radiative transfer equation in participating media with specular reflections using SUPG

- and DG finite elements”, *Journal of Quantitative Spectroscopy and Radiative Transfer*, 179, 149-164, 2016.
- [8] B.G. Carlson, K.D. Lathrop, “Transport theory – the method of discrete ordinates”, *Computing Methods in Reactor Physics*, eds. H. Greenspan, C. N. Kelber, and D. Okrent, Gordon & Breach, New York, 1968.
- [9] M. A. Badri, P. Jolivet, B. Rousseau, S. Le Corre, H. Digonnet, Y. Favennec, “Vectorial finite elements for solving the radiative transfer equation”, *Journal of Quantitative Spectroscopy and Radiative Transfer* 212, 59-74, 2018.
- [10] B. F. Smith, P. Bijørstad, W. Gropp, “Domain decomposition: Parallel Multi-level Methods for Elliptic Partial Differential Equations”, Cambridge University Press, New York, 1996.
- [11] A. Toselli, O.B. Widlund, “Domain Decomposition Methods-Algorithms and Theory”, Springer, Berlin, 2004.
- [12] Y. Saad, M. H. Schultz, “GMRES: A Generalized Minimal Residual Algorithm for Solving Nonsymmetric Linear Systems”, *SIAM Journal on Scientific and Statistical Computing*, 7(3), 856-869, 1986.
- [13] A. St-Cyr, M.J. Gander, S.J. Thomas “Optimized multiplicative, additive and restricted additive Schwarz preconditioning”, *SIAM Journal on Scientific Computing*, 29, 2402-2425, 2017.
- [14] M. J. Gander, “Optimized Schwarz methods”, *SIAM Journal on Numerical Analysis*, 44, 699-731, 2006.
- [15] O. Dubois, “Optimized Schwarz Methods with Robin Conditions for the Advection-Diffusion Equation”, *Domain Decomposition Methods in Science and Engineering XVI*, Springer, 181–188, 2007.
- [16] V. Dolean, S. Lanteri, F. Nataf, “Convergence Analysis of a Schwarz Type Domain Decomposition Method for the Solution of the Euler Equations”, *Applied Numerical Mathematics*, 49(2), 153-186, 2004.